soil systems

MDPI

Article

A Three-Dimensional Assessment of Soil $\delta^{13}C$ in a Subtropical Savanna: Implications for Vegetation Change and Soil Carbon Dynamics

Yong Zhou [1,2], Thomas W. Boutton [1,*] and X. Ben Wu [1]

[1] Department of Ecosystem Science and Management, Texas A&M University, College Station, TX 77843, USA; yong.zhou@yale.edu (Y.Z.); xbw@tamu.edu (X.B.W.)
[2] Department of Ecology and Evolutionary Biology, Yale University, New Haven, CT 06511, USA
* Correspondence: boutton@tamu.edu

Received: 25 September 2019; Accepted: 9 November 2019; Published: 13 November 2019

Abstract: Tree/shrub encroachment into drylands is a geographically widespread vegetation change that often modifies soil organic carbon (SOC) storage and dynamics, and represents an important yet uncertain aspect of the global carbon (C) cycle. We quantified spatial patterns of soil $\delta^{13}C$ to 1.2 m depth in a subtropical savanna to evaluate the magnitude and timing of woody encroachment, and its impacts on SOC dynamics. Woody encroachment dramatically altered soil $\delta^{13}C$ spatial patterns throughout the profile; values were lowest in the interiors of woody patches, increased towards the peripheries of those patches, and reached highest values in the surrounding grasslands. Soil $\delta^{13}C$ and ^{14}C revealed this landscape was once dominated by C_4 grasses. However, a rapid vegetation change occurred during the past 100–200 years, characterized by (1) the formation and expansion of woody patches across this landscape, and (2) increased C_3 forb abundance within remnant grasslands. Tree/shrub encroachment has substantially increased SOC and the proportion of new SOC derived from C_3 plants in the SOC pool. These findings support the emerging perspective that vegetation in many dryland ecosystems is undergoing dramatic and rapid increases in SOC storage, with implications for the C cycle at regional and global scales.

Keywords: woody plant encroachment; spatial patterns; soil $\delta^{13}C$; vegetation change; soil organic carbon dynamics; landscape scale; soil profile; subtropical savanna

1. Introduction

Arid and semiarid regions (drylands) cover approximately 40% of the Earth's land surface [1], and support approximately 20% of the human population [2]. Furthermore, dryland soils store approximately 16% of global soil organic carbon (SOC) and represent an important sink for greenhouse gas emissions [3]. However, carbon (C) cycling processes in dryland ecosystems are particularly sensitive to environmental changes [4], and their responses to climate change and land cover/land use require additional clarification to improve our representations of the C cycle at ecosystem, landscape, and global scales [5].

The increase in woody plant abundance in deserts, grasslands, savannas, and other dryland ecosystems around the world is among the most significant ecological changes occurring globally [6,7]. This vegetation change is likely a response to multiple local and global forcing factors, including the intensification of livestock grazing, reduced fire frequency, elevated atmospheric CO_2 concentration, and changes in the climate system [7–15], and has dramatically altered the dryland C cycle across multiple spatial scales [16–19]. For example, up to 330 million hectares in dryland ecosystems are currently undergoing woody encroachment in the USA alone [17,20], and this conversion appears

to represent 20–40% of the current C sink strength in that country [20–22]. However, field studies assessing woody encroachment effects on SOC pool sizes yield inconsistent results, showing net increase in some dryland ecosystems [19,23–25], but no net change [26], or even decrease in others [18]. These discrepancies may be due to soil chemical and physical characteristics, the quality of organic matter inputs, climate regimes, and/or land use history [16,18,27]. Since vegetation dynamics can have major effects on C cycling in dryland ecosystems [28], a deeper knowledge of the legacy effect of vegetation change on SOC dynamics is important to gauge this uncertainty and to generate more robust predictions of dryland C budgets.

Stable C isotope ratios ($\delta^{13}C$ values) in soils are often used to study vegetation change and SOC dynamics where C_3 plants replace C_4 plants, or vice versa [29–31]. C_3 and C_4 plant species have distinctive $\delta^{13}C$ values in their tissues which are incorporated into soils with relatively little isotope fractionation (1–2‰) during soil organic matter formation [32–36]. Soil $\delta^{13}C$ has been applied to deduce vegetation dynamics on timescales of decades with the aid of aerial photography [37], and on timescales of centuries to millennia in association with soil radiocarbon dating [29,31,38]. In addition, where C_3-C_4 vegetation changes have occurred at known points in time, it has been possible to use the rate at which soil $\delta^{13}C$ values change thereafter to estimate and model SOC turnover and dynamics [39–41].

The encroachment of C_3 woody species into C_4 grass-dominated ecosystems provides an ideal platform for the application of stable C isotopic techniques to address changes in soil C cycling processes following vegetation change. As a result, soil $\delta^{13}C$ values have been used to document and quantify woody expansion [29,38,42], SOC dynamics [40,41], and erosional processes [41,43]. However, most of these prior studies were carried out at the ecosystem scale, limited to relatively shallow soil sampling, and were not spatially explicit. In dryland systems, heterogeneity of tree/shrub cover is the main characteristic of ecosystem structure, and strongly drives ecosystem function and services across multiple spatial scales [44]. In order to cope with this patchiness, we need to explore ecosystem structure and function at larger spatial scales and in a spatially specific manner [45–47]. A few previous studies demonstrated the merits of integrating quantitative spatial analyses and soil $\delta^{13}C$ values to study vegetation dynamics following vegetation change at the landscape scale [37,48,49], but their results were constrained to surface soils. Woody plant encroachment into grass-dominated ecosystems substantially amplifies spatial heterogeneity of soil properties both vertically (through the soil profile) and horizontally (across multiple spatial scales) [19,50]. Despite this, we know little regarding the extent to which spatial patterns of soil $\delta^{13}C$ are affected by increased woody plant abundance in grasslands, particularly at depth in the profile, and how this might influence the soil C cycle in dryland ecosystems.

The primary purpose of this study was to quantitatively characterize the landscape-scale spatial patterns of soil $\delta^{13}C$ throughout the entire soil profile, and relate these spatial patterns to vegetation change and SOC dynamics. To accomplish this, soil samples were collected to a depth of 1.2 m and spatially georeferenced within a subtropical savanna landscape where tree/shrub cover increased dramatically during the past 150 years [29,51]. We tested the hypotheses that: (1) The distribution of woody patches within the grassland matrix would strongly influence spatial patterns of soil $\delta^{13}C$ values across the landscape and throughout the soil profile, (2) these spatial patterns of soil $\delta^{13}C$ will record the pattern of historical vegetation change and reflect the formation and expansion of woody patches in grassland, and (3) grassland to woodland conversion will alter SOC pool sizes and dynamics with respect to C origins in three-dimensional soil space.

2. Materials and Methods

This study was conducted at the Texas A&M AgriLife La Copita Research Area (27°40′ N, 98°12′ W) in the Rio Grande Plains of southern Texas, USA. The climate is subtropical, with a mean annual temperature of 22.4 °C. Mean annual precipitation is 680 mm, with rainfall maxima in May and September. Elevation ranges from 75 to 90 m. Upland surfaces are relatively flat and grade gently

(1–3% slopes) into lower-lying portions of the landscape. The site was grazed at moderate to heavy intensities by livestock from approximately 1880–1985 [52], but has been light since 1985. The research area has not been burned for at least the past 35 years.

The dominant soil on upland portions of the landscape is a sandy loam (Typic Argiustoll, Runge series) with a nearly continuous argillic horizon (B*t*) beginning at approximately 30 cm; however, gaps in the argillic horizon also occur within the uplands [51,53,54], and these soils classify as Aridic Ustochrepts (Saspamco Series) [55,56]. Soil physical characteristics are provided in Supplemental Table S1.

Upland plant communities have a two-phase pattern [57] comprised of patches of trees and shrubs lying within a grassy matrix. Woody patches include small discrete clusters (<10 m in diameter) and large groves (>10 m in diameter). In this region, woody encroachment is initiated when grassland is colonized by *Prosopis glandulosa*, a nitrogen fixing leguminous tree, which then facilitates the recruitment of another 15–20 understory tree and shrub species to form discrete clusters [52]. Where the argillic horizon is absent, discrete clusters continue to grow laterally and fuse together to form large groves [51,53,58]. Thus, discrete clusters and grasslands occur where the argillic horizon is present, while groves occur on soils where the argillic horizon is absent. Woody species composition and relative dominance are similar in both groves and discrete clusters, but individual plants are often larger and older in groves than in discrete clusters [29,46,51]. Herbaceous vegetation is largely absent beneath tree/shrub canopies in clusters and groves. Grasslands, clusters, and groves are each distinct ecosystems characterized by different plant species (Table S2) and soil biogeochemical properties and processes [19,29,59,60], and they represent the most common elements of upland landscapes in this region [61].

Previous studies in this same study area have quantified both the $\delta^{13}C$ values [29] and the concentrations and pools sizes [24] of soil organic carbon. These studies provided valuable insights regarding vegetation dynamics [37,58], soil organic matter densities [62], and mean residence times of soil organic carbon [40]. However, nearly all of these prior studies were based on patch scale sampling (i.e., samples taken within grassland, cluster, and grove ecosystems), and therefore did not provide a spatially specific landscape-scale perspective. One of our prior studies was conducted within this exact same study area utilizing spatially specific landscape-scale soil sampling, but sampling was limited to the upper 15 cm of the soil profile [37,46]. Thus, the spatially specific and relatively deep (1.2 m) soil samples acquired in this study represent a novel dataset that provides a unique three-dimensional assessment of soil $\delta^{13}C$ values and offers new insights regarding our understanding of vegetation change and SOC storage and turnover at the landscape scale.

We utilized a 160 m × 100 m site (Figure 1) that was established in January 2002 on an upland portion of the landscape [37,46]. This 1.6 ha plot was subdivided into 10 m × 10 m grid cells, the corners of which were marked with polyvinyl chloridepoles and georeferenced (Trimble Pathfinder GPS Pro XRS, Trimble Navigation Limited, Sunnyvale, CA, USA) based on the Universal Transverse Mercatorcoordinate system (World Geodetic System (WGS), 1984).

In July 2014, two points were selected randomly for soil sampling in each grid cell, resulting in 320 sample points within the study area (Figure 1b). Vegetation cover at each soil sampling point was classified as grassland (n = 200), cluster (n = 41), or grove (n = 79) based on vegetation type and the canopy size of woody patches. Exact locations of each soil sampling point were determined relative to the georeferenced cell corners. At each soil sampling point, two adjacent soil cores (2.8 cm in diameter and 120 cm in length) were collected. All soil cores were subdivided into 0–5, 5–15, 15–30, 30–50, 50–80, and 80–120 cm depth increments. Leaf and fine root (<2 mm) tissues of all major plant species occurring within the 160 m × 100 m landscape (Table S2) were collected in September 2016.

All soils from one of the two soil cores were dried at 105 °C for 48 h to determine bulk density, then used to isolate fine (<2 mm) and coarse roots (>2 mm) by washing through sieves. It was not possible to discriminate live vs. dead roots. Roots were dried for 48 h at 65 °C and then weighed. To analyze $\delta^{13}C$ of fine roots, 10 cores were selected from each landscape element, and fine roots within

the selected 10 cores were composited for each depth increment. This process was repeated three times to achieve three replicates. Composited fine root samples, as well as the leaf and fine root tissues collected directly from individual plant species present in the study area, were pulverized in a Mixer Mill MM 400 (Retsch GmbH, Haan, Germany), and saved for determination of C concentrations and $\delta^{13}C$ values.

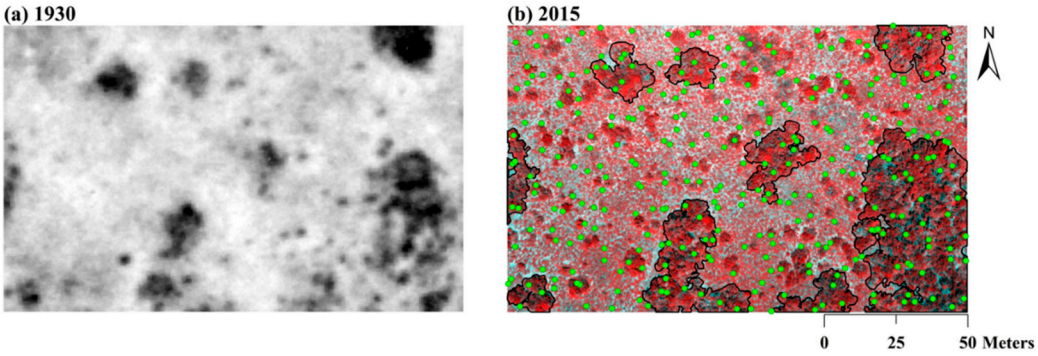

Figure 1. Aerial photographs of the study area from 1930 (**a**) and 2015 (**b**). In the 1930 photo, black areas indicate woody clusters and groves, while lighter grey areas are grassland. In the 2015 photo, dark red areas denote woody clusters and groves, while pink and grey areas represent grassland. Green dots in 2015 indicate the locations of soil samples. Grove edges in 2015 are highlighted with black lines. The 1930 photo was published in Bai et al. (2009) [37] and is reproduced with permission from the American Geophysical Union.

Soils from the other soil core were air-dried and passed through a 2 mm sieve to remove large organic fragments. Aliquots of each sieved soil sample were dried (48 h at 60 °C) and pulverized in a centrifugal mill (Angstrom Inc., Belleville, MI, USA). Samples were weighed into silver capsules (5 mm × 9 mm), treated with HCl vapor in a desiccator to remove carbonates [63], and then dried. SOC concentrations and $\delta^{13}C$ values of acid-treated soil samples were determined using a Costech ECS 4010 elemental analyzer (Costech Analytical Technologies Inc., Valencia, CA, USA) interfaced via a ConFlo IV device with a Delta V Advantage isotope ratio mass spectrometer (Thermo Scientific, Bremen, Germany). The C concentrations and $\delta^{13}C$ values of composited fine root samples, leaf, and fine root tissues of each species were determined similarly, but without acid treatment. Carbon isotope ratios are presented in δ notation:

$$\delta = \left(\frac{R_{Sample} - R_{STD}}{R_{STD}} \right) \times 10^3 \quad (1)$$

where R_{Sample} is the $^{13}C/^{12}C$ ratio of the plant or soil sample and R_{STD} is the $^{13}C/^{12}C$ ratio of the Vienna PeeDee Belemnite (V-PDB) standard. Precision of duplicate measurements was 0.1‰ for $\delta^{13}C$.

The relative proportion of SOC originating from C_3 plants was computed using soil $\delta^{13}C$ values in a simple mass balance mixing model:

$$\delta^{13}C_{soil} = f * \delta^{13}C_3 + (1 - f) * \delta^{13}C_4 \quad (2)$$

where $\delta^{13}C_{Soil}$ is the measured $\delta^{13}C$ value of soil samples, $\delta^{13}C_3$ is the mean $\delta^{13}C$ value of C_3 vegetation, $\delta^{13}C_4$ is the mean $\delta^{13}C$ value of C_4 vegetation, f is the proportion of C derived from C_3 vegetation, and 1-f is the proportion of C derived from C_4 vegetation [29,33]. Averaged $\delta^{13}C$ values of contemporary C_3 and C_4 vegetation are usually used as proxies for past C_3 and C_4 vegetation [29]. Measurements of leaf and fine root tissues in this study yielded average $\delta^{13}C$ values of −28.2‰ (n = 48) and −12.9‰ (n = 26) for C_3 and C_4 vegetation, respectively. These values were applied in Equation (1).

It should be noted that this simple mass balance mixing model may be inexact for two reasons. First, the proportion of C with C_3 origins (or percentage of C_3 vegetation) may be underestimated due to the depth-enrichment of $\delta^{13}C$ throughout the soil profile via several proposed mechanisms which

are independent from vegetation change [33,35,64], including: (1) The decline in the $\delta^{13}C$ value of atmospheric CO_2 due to combustion of ^{13}C-depleted fossil fuels since the beginning of the Industrial Revolution (the Suess effect), (2) microbial isotope discrimination during decomposition, and (3) adsorption of ^{13}C-enriched microbial residues to fine mineral particles. Soil $\delta^{13}C$ enrichment from the soil surface to deeper in the profile is usually between 1–3‰ [35]; isotopic changes larger than this are likely attributable to a shift from C_3 to C_4 vegetation. Second, there is evidence suggesting that SOC inputs from C_4 plants decompose more rapidly than those derived from C_3 plants [65–67] potentially resulting in lower soil $\delta^{13}C$ values that yield overestimates of the relative proportion of SOC derived from C_3 plants. Thus, there appears to be some environmental factors that could yield underestimates of C_3-derived SOC, and others that might cause overestimates of C_3-derived SOC. However, the data collected in this study do not allow us to evaluate the net influence of these factors on our $\delta^{13}C$ values or our estimates of the proportions of SOC derived from C_3 vs. C_4 sources.

Datasets deviating from normality were log-transformed. A mixed model was used to compare soil variables (i.e., soil $\delta^{13}C$, SOC concentration, and % C derived from C_3 vegetation) in different landscape elements. In the mixed model, spatial autocorrelation was considered as a spatial covariance for adjustment [68]. Differences in $\delta^{13}C$ values of leaf and fine root tissues in different plant life forms and of composited fine root samples in different landscape elements were assessed using one-way ANOVAs. Post hoc comparisons of these variables were conducted using Tukey's correction. All statistical analyses were performed in JMP Pro 12.0 (SAS Institute Inc., Cary, NC, USA).

A sample variogram fitted with a variogram model was developed to quantify the spatial structure of soil $\delta^{13}C$ in each depth increment using R [69]. Ordinary kriging based on the best fitted variogram model was used to predict soil $\delta^{13}C$ values at unsampled locations for each soil depth increment. A kriged map of soil $\delta^{13}C$ for each depth increment was generated in ArcMap 10.2.2 (ESRI, Redlands, CA, USA) using the Spatial Analyst tool. Kriged maps of percentage (%) of C derived from C_3 vegetation were generated for each soil depth increment in the same way. Woody patches in aerial photographs of this landscape taken in 1930 and 2015 were digitized and areas of each woody patch were calculated in ArcMap 10.2.2. (ESRI, Redlands, CA, USA). To evaluate spatial trends from the centers of woody patches to the grassland matrix, the distance from each sampling point to the nearest woody patch edge was calculated and correlated with soil $\delta^{13}C$. Sample points located in woody patches were assigned positive distances such that larger values indicated sampling points were closer to the centers of woody patches. In contrast, samples located in the grassland matrix were assigned negative distances; thus, more negative values indicated that sample points were more distant from the edges of woody patches.

3. Results

3.1. Woody Plant Encroachment Altered Spatial Patterns of Soil $\delta^{13}C$ throughout the Soil Profile

Mean $\delta^{13}C$ values of woody plant tissues (leaves = −28.9‰, fine roots = −27.2‰) were similar to those for forbs (leaves = −29.4‰, fine roots = −27.7‰) (Figure 2, Table S2). C_3 woody plants and forbs had significant lower mean $\delta^{13}C$ values in leaf and fine root tissues than C_4 grasses (leaves = −14.1‰, fine roots = −13.4‰) (Figure 2, Table S2). Fine roots had slightly higher $\delta^{13}C$ values than leaf tissues (Figure 2, Table S2) for all life-forms. Composited fine root samples from both clusters and groves (woody patches, hereafter) had $\delta^{13}C$ values (−27 to −26‰) significantly lower than those from grasslands (−22.5 to −20.9‰) throughout the entire profile (Figure 3). The $\delta^{13}C$ of composited fine root samples from woody patches were relatively constant with depth, while those from grasslands decreased slightly with soil depth (Figure 3).

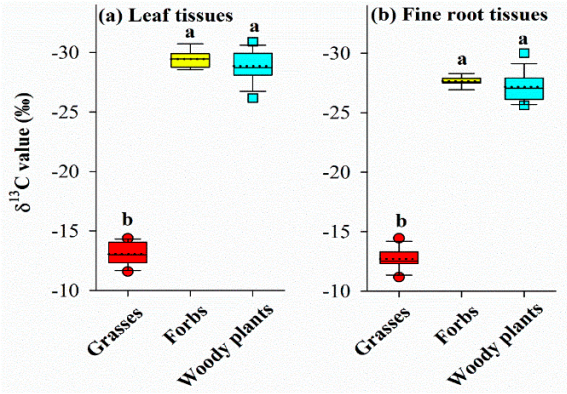

Figure 2. The $\delta^{13}C$ values (‰) of leaf (**a**) and fine root (**b**) tissues for different plant life forms occurring on the landscape. Box plots summarize the distribution of points for each variable within each plant life form. The central box shows the interquartile range, median (horizontal solid line in the box), and mean (horizontal dotted line in the box). Lower and upper error bars indicate 10th and 90th percentiles, and points above or below the error bars are individuals above the 90th or below the 10th percentiles. Number of samples: Grasses, n = 13; forbs, n = 9; woody plants, n = 15. For more details, see Table S2.

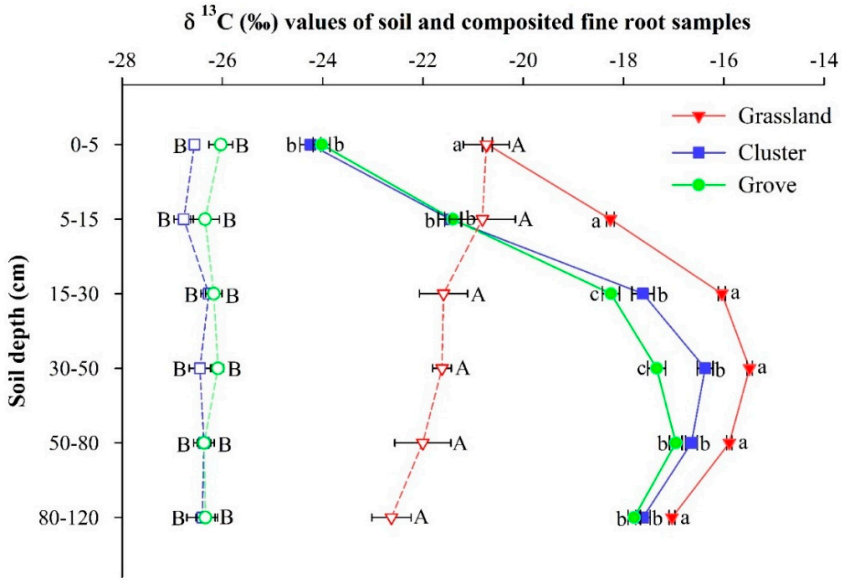

Figure 3. The $\delta^{13}C$ values (‰) of soil (solid symbols, solid lines) and composited fine root samples (hollow symbols, dashed lines) for grasslands, clusters, and groves throughout the 1.2 m profile. Significant differences ($p < 0.05$) between means of landscape elements are indicated with uppercase letters for fine root samples, and lowercase letters for soil samples. Number of soil samples: Grassland = 200, cluster = 41, and grove = 79. The $\delta^{13}C$ values (‰) of composited fine root samples for different landscape elements are based on three replicates.

Woody patches had significantly lower soil $\delta^{13}C$ values than grasslands throughout the soil profile. Soil $\delta^{13}C$ values were significantly lower in groves than clusters, but only in the 15–30 and 30–50 cm depth increments (Figure 3). Soil $\delta^{13}C$ values increased with soil depth, reached maximum values between 30–80 cm depth increments, and then decreased slightly in the deeper increments (Figure 3).

The kriged maps indicated that soil $\delta^{13}C$ values were lowest in the centers of woody patches (especially for groves), increased towards the boundaries of woody patches, and reached maximum values within the surrounding grassland (Figure 4a–g). This spatial trend apparent in the kriged maps was supported by significant negative correlations between soil $\delta^{13}C$ and distance from each sampling point to the nearest woody patch edge throughout the soil profile (Figure 5). However, this spatial

pattern of soil $\delta^{13}C$ gradually weakened with soil depth (Figure 4a–g). Statistically, the slopes of correlations between soil $\delta^{13}C$ and distance from each sampling point to the nearest woody patch edge became lower - with soil depth, and the strengths of these relationships (R^2) also weakened with soil depth (Figure 5). In addition, the coefficient of variation (CV) of soil $\delta^{13}C$ across this landscape decreased with soil depth from 9.78% in the 0–5 cm increment to 5.57% in the 80–120 cm depth increment (Table S3). Collectively, these results indicate the reduced impact of woody plant encroachment on the spatial variation of soil $\delta^{13}C$ in deeper portions of the soil profile across this landscape.

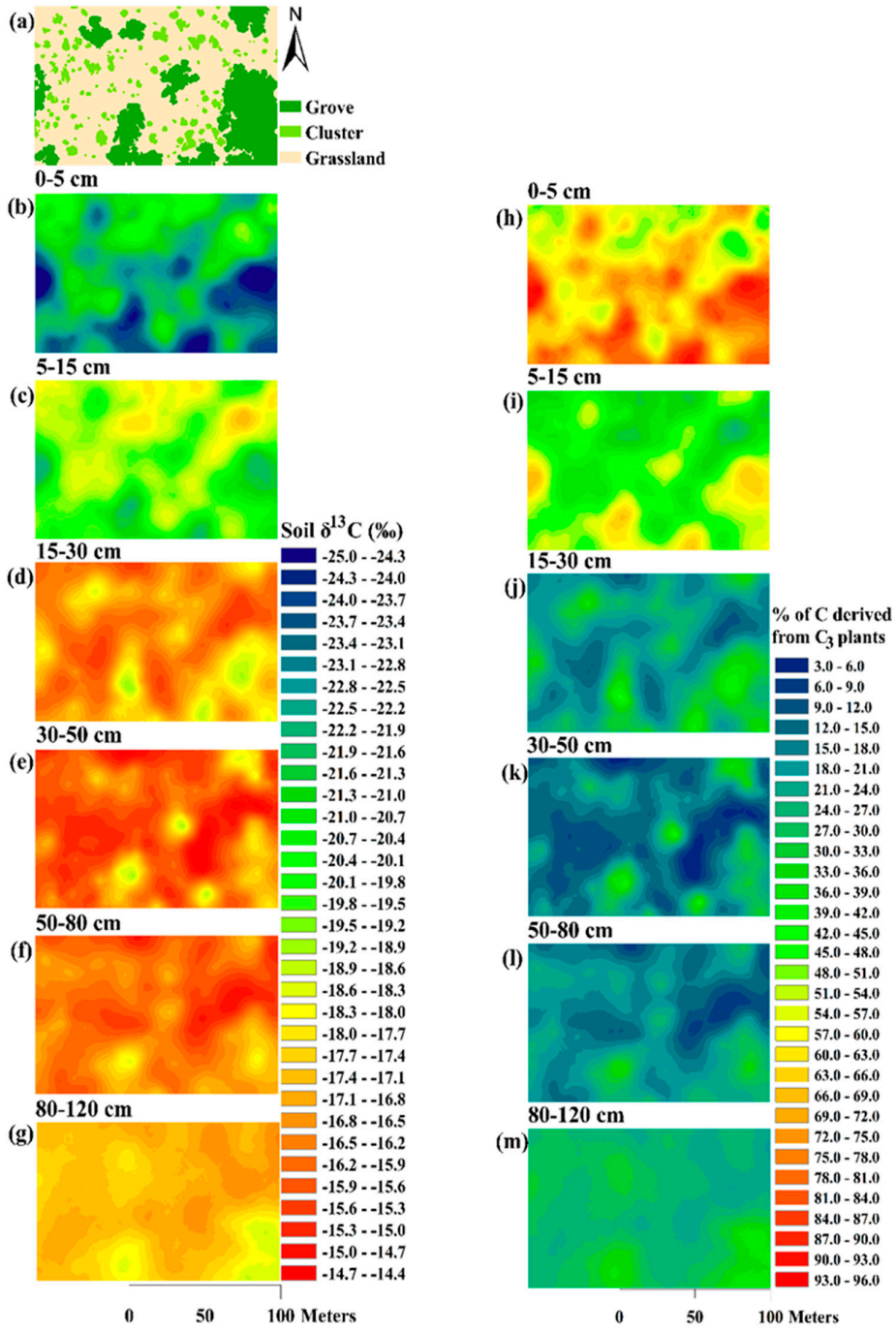

Figure 4. Classified vegetation map based on aerial photograph taken in 2015 (**a**) and kriged maps of soil $\delta^{13}C$ values (‰) (**b**–**g**) and % of C derived from C_3 plants (**h**–**m**) across this 1.6 ha landscape and in each soil depth increment.

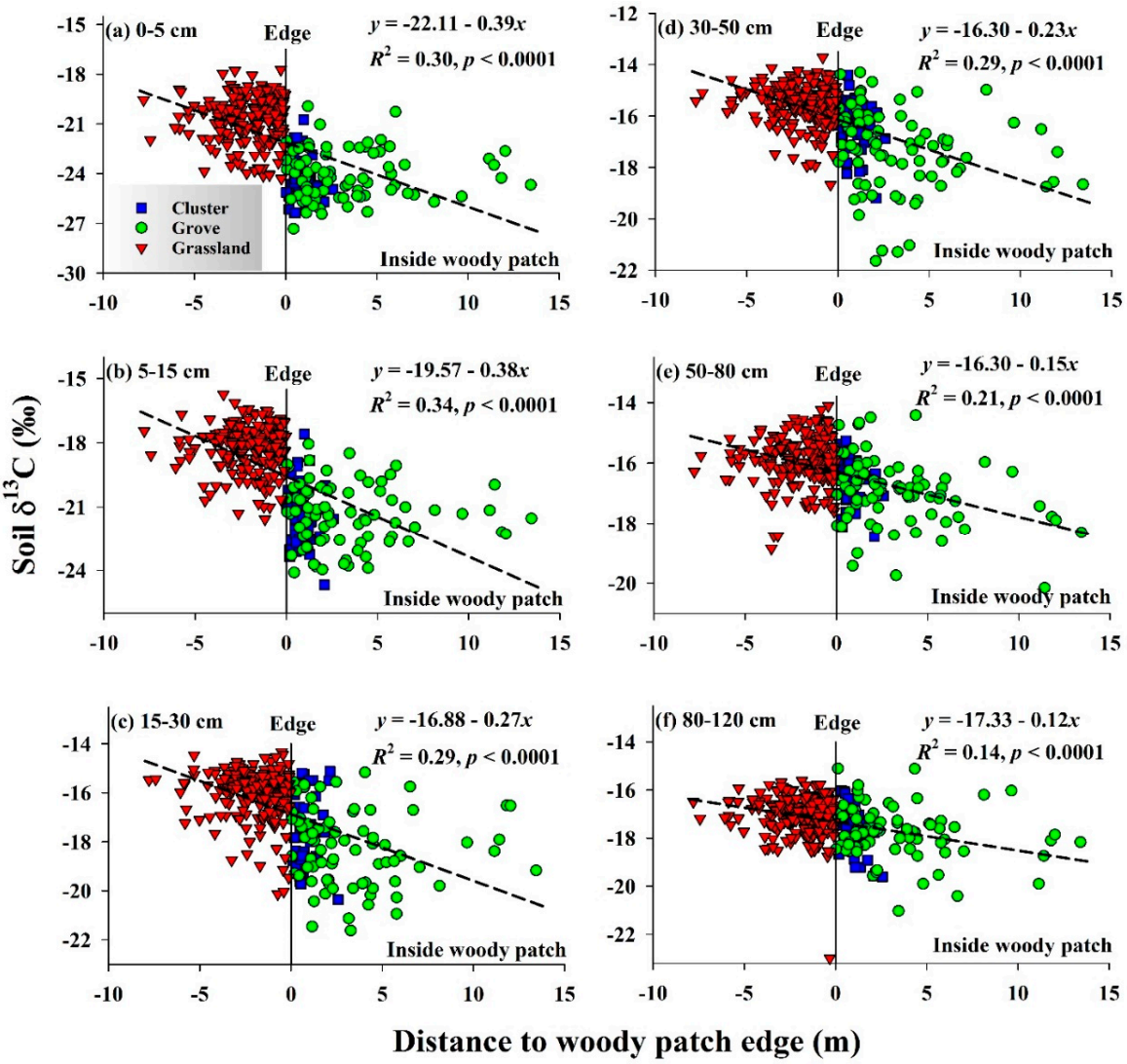

Figure 5. Correlations between soil $\delta^{13}C$ values (‰) and distance (m) of each sampling point to the nearest woody patch boundary within each depth increment (panels **a**–**f**). Distances >0 indicate sample points within woody patches, whereas distances <0 indicate sample points within the grassland.

3.2. Vegetation Changes Based on Spatial Patterns of Soil $\delta^{13}C$

In clusters and groves, $\delta^{13}C$ values of fine roots (−27 to −26‰) throughout the soil profile were entirely consistent with known values for C_3 plants (Figures 2 and 3). In the 0–5 cm depth interval of those same landscape elements, $\delta^{13}C$ values of SOC (−24‰) approached those of fine roots, suggesting most of the SOC in that depth interval was derived from the current C_3 woody plant cover. However, at depths between 5–120 cm, $\delta^{13}C$ values of SOC were much higher (−21.5 to −16.5‰) than those of the associated fine roots, and indicated that only approximately 23 to 56% of the SOC at depths >5 cm was derived from C_3 plant sources (Table 1). These patterns indicate that clusters and groves must be relatively recent components of this landscape.

In grasslands, $\delta^{13}C$ values of fine roots decreased gradually from −20.9‰ at 0–5 cm to −22.5‰ at 80–120 cm (Figure 3). While $\delta^{13}C$ values of fine roots and SOC were similar at 0–5 cm, the $\delta^{13}C$ values of SOC were 3 to 6‰ greater than those of fine roots at depths >5 cm. These data indicate that approximately 51% of SOC in the 0–5 cm depth interval was derived from C_3 plants, while 17 to 35% of SOC was from C_3 sources at depths >5 cm (Table 1). The large isotopic disequilibrium between fine roots and SOC in grasslands indicates that the grasslands were once more C_4-dominated than they are currently.

Table 1. Soil organic carbon (SOC) concentration (g C kg^{-1} soil), percentage (%) of SOC derived from C_3 plants, and percentage (%) of new SOC derived from woody plants in grasslands, clusters, and groves. Significant differences between landscape elements are indicated with different superscript letters. Values are means ± standard errors (SE). Number of samples: Grassland = 200, cluster = 41, and grove = 79.

Depth (cm)	SOC (g C kg^{-1} soil) *			% SOC Derived from C_3 Plants			% of New SOC Derived from Woody Plants **	
	Grassland	Cluster	Grove	Grassland	Cluster	Grove	Cluster	Grove
0–5	6.7 ± 0.1 ^{c}	17.0 ± 1.4 ^{b}	22.1 ± 1.4 ^{a}	51.1 ± 0.6 ^{b}	74.2 ± 1.4 ^{a}	72.7 ± 1.1 ^{a}	60.5 ± 3.6 ^{a}	62.3 ± 3.1 ^{a}
5–15	5.4 ± 0.1 ^{b}	8.2 ± 0.5 ^{a}	8.8 ± 0.3 ^{a}	35.1 ± 0.5 ^{b}	55.9 ± 1.5 ^{a}	55.6 ± 1.1 ^{a}	37.6 ± 2.8 ^{a}	38.9 ± 2.0 ^{a}
15–30	5.1 ± 0.0 ^{b}	6.0 ± 0.2 ^{a}	6.3 ± 0.1 ^{a}	20.5 ± 0.5 ^{c}	30.8 ± 1.5 ^{b}	35.0 ± 1.1 ^{a}	15.4 ± 2.2 ^{b}	21.8 ± 1.7 ^{a}
30–50	5.0 ± 0.1 ^{a}	5.3 ± 0.1 ^{a}	5.3 ± 0.1 ^{a}	16.9 ± 0.4 ^{c}	22.7 ± 1.0 ^{b}	29.0 ± 1.2 ^{a}	8.0 ± 1.4 ^{b}	17.4 ± 1.7 ^{a}
50–80	3.5 ± 0.0 ^{b}	3.9 ± 0.1 ^{a}	3.9 ± 0.1 ^{a}	19.5 ± 0.4 ^{b}	24.5 ± 0.8 ^{a}	26.5 ± 0.8 ^{a}	7.2 ± 1.1 ^{a}	10.2 ± 1.2 ^{a}
80–120	2.3 ± 0.0 ^{b}	2.6 ± 0.1 ^{a}	2.9 ± 0.1 ^{a}	27.0 ± 0.4 ^{b}	30.8 ± 0.9 ^{a}	32.0 ± 0.8 ^{a}	6.5 ± 1.5 ^{a}	8.4 ± 1.3 ^{a}

* Data from Zhou et al. [60]. ** Data from Zhou et al. [50].

Although the exact time at which woody species began to encroach into this landscape remains unknown, a comparison of aerial photographs taken in 1930 and 2015 (Figure 1a,b) provides some chronological perspective. Raster calculations showed that total woody cover for the 160 m × 100 m landscape increased 16.7% (2672 m^2) during the past 85 years (Table 2, Figure 1a,b). All groves identified in the aerial photograph taken in 2015 were already present in the 1930 aerial photo (Figure 1a,b); however, the grove cover across this landscape increased from 2649 m^2 to 4375 m^2, accounting for 10.7% of the increase in total woody cover (Table 2). Compared to 1930, 89 new clusters were identified in the aerial photograph taken in 2015 (data not shown). This leads to an increase of cluster cover from 693 m^2 to 1649 m^2, accounting for 6.0% of the increase in total woody cover (Table 2).

Table 2. Woody plant cover changes from 1930 to 2015 for the 100 m × 160 m landscape assessed from aerial photography.

Time	Grove Cover		Cluster Cover		Total Woody Cover	
	m^2	%	m^2	%	m^2	%
1930	2659	16.6	693	4.3	3352	20.9
2015	4375	27.3	1647	10.3	6024	37.6
Net change (1930–2015)	+1716	+10.7	+956	+6.0	+2672	+16.7

3.3. SOC Sources Inferred from Spatial Patterns of Soil $\delta^{13}C$

SOC concentrations in clusters and groves were higher than those in grasslands (Table 1), and were correlated negatively with soil $\delta^{13}C$ values throughout the soil profile (Figure 6). These relationships were exponential in the 0–5 and 5–15 cm depth intervals, but became linear at depths >15 cm (Figure 6). Soil $\delta^{13}C$ values were generally intermediate between values characteristic of contemporary C_3 and C_4 plants (Figure 2a,b and Figure 3), indicating SOC was derived from a mixture of both C_3 and C_4 sources. Proportions of SOC derived from C_3 sources underneath woody patches were significantly higher than those underneath grasslands throughout the entire soil profile (Table 1), and much of this C_3-derived C originated from woody plants, especially in the uppermost 15 cm of the profile (Table 1). In grasslands, approximately 50% of the SOC was derived from C_3 forbs in the 0–5 cm depth increment (Table 1). Spatial patterns of the proportion of SOC derived from C_3 plants were reversed from those of soil $\delta^{13}C$, and showed higher values inside the woody patches and lower values in the remnant grassland matrix throughout the soil profile (Figure 4h–m).

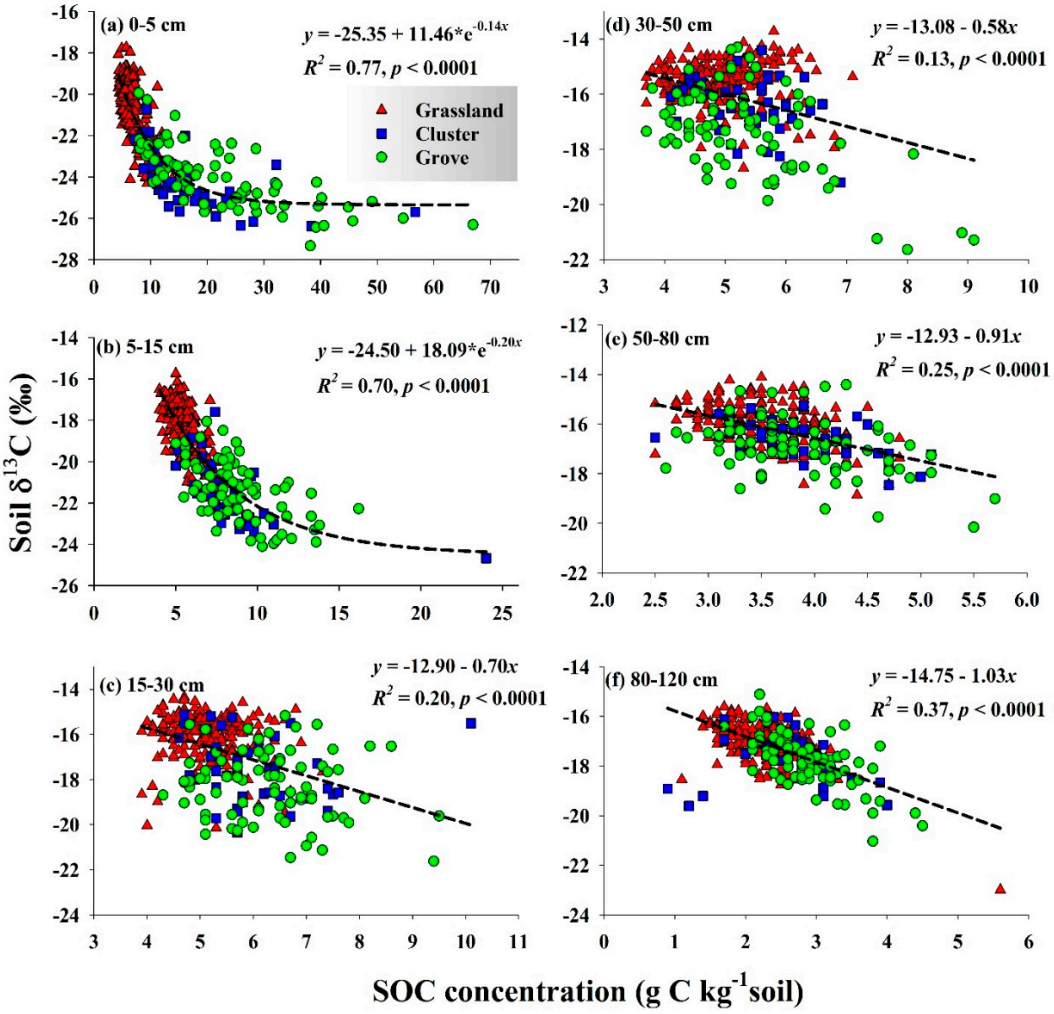

Figure 6. Correlations between soil $\delta^{13}C$ (‰) and SOC concentration (g C kg^{-1} soil) at the 0–5 (**a**), 5–15 (**b**), 15–30 (**c**), 30–50 (**d**), 50–80 (**e**), and 80–120 cm (**f**) depths within the soil profile. Note that scales are different for both x and y axes.

4. Discussion

The increased abundance of C_3 trees and shrubs into the original C_4 grassland delivers ^{13}C-depleted plant materials to soils (Figure 2a,b and Figure 3), altering patterns of spatial heterogeneity in soil $\delta^{13}C$ throughout the soil profile. This alteration is particularly evident in the 0–15 cm depth interval (surface soils, hereafter) where spatial patterns of soil $\delta^{13}C$ resembled strongly the current plant community cover across the landscape, especially the spatial distribution of groves (Figure 4a–g). The $\delta^{13}C$ values of SOC in surface soils gradually increased from the center to the edge of woody patches, and reached highest $\delta^{13}C$ in the grassland matrix (Figures 4a–g and 5). This spatial trend is due to the fact that woody plants near the centers of groves and clusters are older than those near the woody patch-grassland boundary [29,52]; thus, soils near the middle of woody patches have been accumulating ^{13}C-depleted woody plant residues for a longer duration than soils near the edges of the woody patches [19,58,70]. These results are in accord with prior studies showing that changes in C_3-C_4 dominance of plant communities alter surface soil $\delta^{13}C$ across multiple spatial scales [37,48,49,58].

Our results also show that changes in soil $\delta^{13}C$ spatial patterns were evident to a depth of 1.2 m following the conversion from grasslands to woody patches, although to a lesser extent deeper in the soil profile (Figures 4b–g and 5, Table S3). The gradually diminishing influence of woody encroachment on spatial patterns of $\delta^{13}C$ deep in the soil profile is likely due to the fact that: (1) Root biomass, as the primary source of SOC [71–73], decreases exponentially with soil depth as shown in this (Figure S1)

and other studies [19,74]; and (2) soil $\delta^{13}C$ was significantly negatively correlated with root density (kg m^{-3}) throughout the profile (Figure S2). Despite such dramatic decreases with depth, mean root densities of woody patches were still twice as large as those of grasslands in the 80–120 cm soil depth interval (Figure S1), as woody species in dryland ecosystems generally have greater rooting depths than grass species [75]. The deposition of ^{13}C-depleted organic matter via root turnover of woody species, though in reduced quantity in subsurface soils, has nonetheless differentiated soil $\delta^{13}C$ between woody patches and grasslands (Figure 3) and amplified patterns of spatial heterogeneity in $\delta^{13}C$ of subsurface soils across this landscape (Figure 4b–g). These findings emphasize the importance of studying biogeochemical properties and processes in subsurface soils, particularly when changes in rooting characteristics accompany vegetation changes.

The $\delta^{13}C$ values of SOC indicate that vegetation changes have occurred across this entire landscape. The dramatic increase in soil $\delta^{13}C$ from the 0–5 to 15–30 cm soil depth increment under woody patches (Figure 3) and the fact that most of the new C derived from C_3 woody plants is concentrated in surface soils (Table 1) suggest that woody patches are recent components of this landscape. This inference is well supported by the facts that: (1) radiocarbon-derived mean residence times for SOC are 52 yrs and 280 yrs for the 0–15 and 15–30 cm depth increments, respectively [29]; and (2) tree-ring analyses indicate that the maximum ages of dominant trees (i.e., *P. glandulosa*) found in groves and clusters are <130 yrs [24,29,76]. Raster calculations based on aerial photographs taken in 1930 and 2015 indicate that groves are actively expanding and clusters are continuously forming across this landscape (Figure 1a,b, Table 2). Simulations based on transition probabilities [51] and spatial analyses of subsurface soil texture [53] also suggest that the current landscape is in a transitional stage in the succession from grasslands to closed-canopy woodlands. The dramatic increase in woody cover observed in this site is consistent with other studies suggesting that woody plant encroachment is a globally extensive phenomenon in arid and semiarid regions [6,7,14,17].

Isotopic measurements indicate that the grassland component of this landscape has been dynamic as well. In grasslands, $\delta^{13}C$ values of subsurface soils (>15 cm) (−17.0 to −15.5‰, Figure 3) are comparable to average $\delta^{13}C$ values of SOC in soils covered by pure C_4 grass communities (−16.1 ± 2.2‰) throughout the world, as summarized by Victoria et al. (1995) [31]. Our simple mass balance mixing model revealed that the relative proportion of SOC derived from C_3 plants in subsurface soils was less than 27% (Table 1), strongly suggesting that this landscape was once dominated primarily by C_4 grasses. Previous radiocarbon measurements at this same site show that this subsurface soil carbon has mean residence times ranging from 270 ± 40 yrs at 15–30 cm to 1480 ± 35 yrs at 90–120 cm [29], indicating that this landscape was strongly C_4-dominated prior to approximately 200 yrs ago. However, $\delta^{13}C$ values of SOC in the surface soil were −20.7‰ at 0–5 cm and −18.2‰ at 5–15 cm, indicating that 35–51% of SOC was C_3-derived at these depths. The SOC mean residence time derived from radiocarbon measurements was 75 ± 4 yrs for the 0–15 cm soil depth [29]. This isotopic shift in grassland surface soils can only be attributed to an increase in C_3 forbs because C_3 grasses are not a component of the grassland flora at this site, and because the root systems of trees/shrubs within clusters and groves do not extend more than 2 m beyond the woody patch boundaries [54]. Collectively, these $\delta^{13}C$ and ^{14}C measurements show that grasslands in this study area have experienced an increase in C_3 plant species inputs within the last 75–200 yrs. This estimate is coincident with historical accounts indicating this site has been grazed continuously by domestic livestock since the mid to late 1800s [51,52]. Since cattle in this region feed preferentially on C_4 grasses, this gives co-occurring C_3 forbs (many of which are unpalatable) a competitive advantage and allows them to increase their biomass and productivity within the grassland matrix [29,77,78].

It should be recognized that inferences regarding C_3-C_4 vegetation changes derived from soil radiocarbon and $\delta^{13}C$ values can be problematic, and may be affected by: (1) The gradual increase of soil $\delta^{13}C$ with increasing soil depth due to organic matter decay [33,35,64], (2) the possibility that some C_3 forbs in the contemporary vegetation might be deep-rooted and capable of depositing ^{13}C-depleted soil organic matter in subsurface soils (Figure 3), and (3) the difficulty of obtaining accurate estimates of

soil ages [79]. However, these results provide a record of vegetation change that is broadly consistent with historical records, aerial photos from the 1930s to the present, and the ages of the trees that currently dominate wooded areas [29].

Although our prior studies [29,52] indicate that woody encroachment in this region began approximately 150 yrs ago, it is difficult to isolate a single mechanism as the primary cause. This vegetation change coincides temporally with the onset of heavy livestock grazing and reduced fire frequency in the area [51,52], both of which simultaneously created a competitive imbalance favoring woody plants over grasses. However, atmospheric CO_2 concentrations began rising exponentially from 290 ppm in 1880 to 410 ppm today. Since C_3 plants generally have higher photosynthetic rates and water use efficiencies under elevated CO_2 while C_4 plants are less responsive [80], this change in atmospheric composition could also be a factor favoring the physiological performance of C_3 woody plants to a greater extent than C_4 grasses [6,8,9,13]. In addition, both mean annual rainfall and mean annual temperature have increased at our study area between the years 1890–2019. During that time interval, mean annual rainfall increased by approximately 7 mm per decade from 625 to 700 mm yr^{-1}, and mean annual temperature increased by approximately 0.1 °C per decade from 21.4 °C to 22.7 °C [81]. Several other studies have found evidence that woody encroachment is favored by greater precipitation [10,82]. Hence, livestock grazing, reduced fire frequencies, elevated CO_2, and climate change are each powerful environmental forcing factors that have become increasingly important during the past 150 yrs, and have likely interacted to influence tree-grass dynamics at ecosystem to regional scales [83].

Our data have also demonstrated that this dramatic vegetation change from relatively open C_4 grassland to a savanna parkland configuration during the past 150 yrs has significantly impacted SOC storage and dynamics. The increasing abundance of both woody plants and forbs has increased the proportion of C derived from C_3 vegetation (Table 1) and altered the three-dimensional spatial patterns of SOC derived from C_3 plants across the landscape and throughout the soil profile (Figure 4h–m). Though the inherent lability of C_3 vs. C_4 biomass inputs is still unclear, C derived from C_3 vegetation appears to decompose more slowly than that derived from C_4 plants in mixed C_3-C_4 soils due mainly to lignin content and/or mean size of particulate organic matter [65,67]. Previous studies at this site also revealed that grassland to woodland conversion increased the proportions of biochemically recalcitrant lignin subunits and aliphatic compounds present in SOC [62,84,85]. Thus, SOC sequestration potential per unit of organic matter input might be higher for C_3 woody vegetation compared to C_4 grasslands.

In order to further interpret the observed increases in SOC concentration under woody patches, we separated the SOC pool into proportions of new C derived from woody plants vs. old C with herbaceous origins using a mass balance approach [19]. Though substantial proportions of SOC derived from woody plants were observed throughout the soil profile, new C derived from woody plants was concentrated in surface soils (Table 1). Previous studies using a chronosequence approach with an age series of woody patches at this study site found that SOC concentrations in surface soils increased linearly at 10–30 g C m^{-2} yr^{-1} with increasing stand age over durations exceeding 100 years [24,86]; and, dynamic simulation models have predicted that it may take ca. 400 yrs after woody plant encroachment for SOC saturation in surface soils [87]. In addition, no evidence for SOC saturation in surface soils following woody proliferation has been demonstrated in other ecosystems [23,70]. Thus, it is likely that newer C derived from woody plants will continue to accumulate in surface soils as existing woody patches grow older and expand, and as new patches develop on the landscape. The exponential relationships between soil $\delta^{13}C$ and SOC concentration in surface soils also indicate that soils in woody patches have not yet reached the maximum for SOC or the minimum for $\delta^{13}C$ (Figure 6). In contrast, soil $\delta^{13}C$ and SOC concentration in subsurface soils were linearly related (Figure 6) and new C derived from woody plants represented <20% of the SOC pool (Table 1), suggesting that subsurface soils have great potential to accumulate new C derived from woody plants [19]. As most previous studies have focused on surface soils only [16,23–25,27], results from this study suggest that woody

encroachment into grasslands and other dryland ecosystems may represent an even larger sink for atmospheric CO_2 when the potential for SOC sequestration in subsurface soils is considered [19].

Woody plant cover is now increasing at rates of 0.1 to 2.3% yr^{-1} in grasslands, savannas, deserts, and other dryland ecosystem types throughout the world [6,16], and often has significant ecological, economic, and cultural impacts [7]. However, efforts to restore encroached systems back to their original grass-dominated configuration may be hampered by significant ecological and environmental changes at ecosystem and global scales that have occurred simultaneously with woody encroachment. For example, rising temperatures, altered rainfall regimes, and increasing atmospheric CO_2 concentrations may differentially affect competitive abilities of C_3 woody plants and C_4 grasses [8–11,80,83]. These global changes may override or hamper local management efforts aimed at restoring grasslands. In addition, woody encroachment often dramatically alters belowground ecosystem properties such as root biomass and distribution patterns [54], C and nutrient storage and dynamics [16,17,19,27,40], the size and activity of the soil microbial biomass pool [88], and the biodiversity and metabolic potential of soil microbial and animal communities [89–91]. Collectively, these profound global and ecosystem scale changes may be externally and internally reinforcing the woody encroached state, making it difficult to restore encroached ecosystems back to the grass-dominated configurations that once dominated these areas. In fact, most efforts to reduce woody cover achieve limited success and the results are short-lived and generally persist for <10 yrs, indicating that woody-encroached grasslands are alternate stable states [7]. Although considerable effort has been invested to understand the ecological causes and consequences of globally widespread woody plant encroachment into grass-dominated ecosystems, there is now growing recognition that we need to broaden our perspectives and approach woody encroachment as a social-ecological phenomenon in order to enhance our ability to adapt to, prevent, reverse, or otherwise manage this ongoing land cover change [92,93].

5. Conclusions

Vegetation dynamics across this landscape, especially the encroachment of C_3 woody plants into the remnant grassland matrix, have created a heterogeneous landscape structure that is reflected in the spatial variation of soil $\delta^{13}C$ throughout the soil profile. Results from this subtropical savanna, which may be analogous to other dryland ecosystems in southwestern U.S., Africa, South America, and Australia, showed that vegetation across this landscape is experiencing dramatic changes characterized by a significant increase in abundance of both C_3 woody plants and forbs in a system that was once dominated primarily by C_4 grasses. While there are uncertainties regarding the impact of woody encroachment on SOC storage, our results show that SOC has increased significantly following encroachment, and we provide $\delta^{13}C$ evidence to show that this new SOC accrual is derived from C_3 woody plants. Although most of the SOC derived from woody plants has accrued in the upper 30 cm of the profile, new woody plant carbon could be readily identified throughout the entire 1.2 m soil profile, emphasizing the importance of quantifying deep-soil C following ecosystem change. Given the geographic extent of woody encroachment at the global scale, we suggest that this vegetation change has important implications for predicting and modeling soil C dynamics in dryland regions.

Supplementary Materials: The following are available online at http://www.mdpi.com/2571-8789/3/4/73/s1: Figure S1, root densities (kg m^{-3}) within landscape elements to a depth of 1 m; Figure S2, relationships between soil $\delta^{13}C$ (‰) and root density throughout the soil profile; Table S1, soil physical characteristics and root densities for grasslands, clusters, and groves; Table S2, $\delta^{13}C$ values (‰) of leaf and fine root tissues of dominant plant species across the 160 m × 100 m landscape in a subtropical savanna ecosystem; Table S3, descriptive statistics for all soil $\delta^{13}C$ values (‰) across the 160 m × 100 m landscape within each depth increment.

Author Contributions: Y.Z., T.W.B., and X.B.W. conceived and designed the experiments; Y.Z. performed the experiments, prepared figures and/or tables, and wrote the first draft of the paper; all authors contributed to revisions and approved the final submission.

Funding: This work was funded by a Doctoral Dissertation Improvement Grant from the U.S. National Science Foundation (DEB/DDIG 1600790), USDA/NIFA Hatch Project (1003961), a Howard McCarley Student Research Award from the Southwestern Association of Naturalists, and an Exploration Fund Grant from the Explorers

Club. The funders had no role in study design, data collection and analysis, decision to publish, or preparation of the manuscript.

Acknowledgments: Yong Zhou was supported by a Sid Kyle Graduate Merit Assistantship from the Department of Ecosystem Science and Management and a Tom Slick Graduate Research Fellowship from the College of Agriculture and Life Sciences, Texas A&M University. We thank Ayumi Hyodo for technical support in the Stable Isotopes for Biosphere Sciences Lab at Texas A&M University, and David and Stacy McKown for on-site logistics at the La Copita Research Area.

Conflicts of Interest: The authors declare no conflict of interest.

References

1. Bailey, R.G. *Ecosystem Geography: From Ecoregions to Sites*; Springer: New York, NY, USA, 2009.
2. Jordan, M.; Meyer, W.B.; Kates, R.W.; Clark, W.C.; Richards, J.F.; Turner, B.L.; Mathews, J.T. *The Earth as Transformed by Human Action: Global and Regional Changes in the Biosphere over the Past 300 Years*; Cambridge University Press: Cambridge, UK, 1993.
3. Lal, R. Carbon sequestration in dryland ecosystems. *Environ. Manag.* **2004**, *33*, 528–544. [CrossRef] [PubMed]
4. Delgado-Baquerizo, M.; Maestre, F.T.; Gallardol, A.; Bowker, M.A.; Wallenstein, M.D.; Quero, J.L.; Ochoa, V.; Gozalo, B.; Garcia-Gomez, M.; Soliveres, S.; et al. Decoupling of soil nutrient cycles as a function of aridity in global drylands. *Nature* **2013**, *502*, 672–676. [CrossRef] [PubMed]
5. Poulter, B.; Frank, D.; Ciais, P.; Myneni, R.B.; Andela, N.; Bi, J.; Broquet, G.; Canadell, J.G.; Chevallier, F.; Liu, Y.Y.; et al. Contribution of semi-arid ecosystems to interannual variability of the global carbon cycle. *Nature* **2014**, *509*, 600–603. [CrossRef] [PubMed]
6. Stevens, N.; Lehmann, C.E.R.; Murphy, B.P.; Durigan, G. Savanna woody encroachment is widespread across three continents. *Glob. Chang. Biol.* **2017**, *23*, 235–244. [CrossRef] [PubMed]
7. Archer, S.R.; Andersen, E.M.; Predick, K.I.; Schwinning, S.; Steidl, R.J.; Woods, S.R. Woody plant encroachment: Causes and consequences. In *Rangeland Systems*; Springer Nature: Cham, Switzerland, 2017; pp. 25–84. [CrossRef]
8. Bond, W.J.; Midgley, G.F. Carbon dioxide and the uneasy interactions of trees and savannah grasses. *Phil. Trans. R. Soc. B* **2012**, *367*, 601–612. [CrossRef] [PubMed]
9. Devine, A.P.; McDonald, R.A.; Quaife, T.; Maclean, I.M.D. Determinants of woody encroachment and cover in African savannas. *Oecologia* **2017**, *183*, 939–951. [CrossRef]
10. Kulmatiski, A.; Beard, K.H. Woody plant encroachment facilitated by increased precipitation intensity. *Nat. Clim. Chang.* **2013**, *3*, 833–837. [CrossRef]
11. Morgan, J.A.; Milchunas, D.G.; LeCain, D.R.; West, M.; Mosier, A.R. Carbon dioxide enrichment alters plant community structure and accelerates shrub growth in the shortgrass steppe. *Proc. Nat. Acad. Sci. USA* **2007**, *104*, 14724–14729. [CrossRef]
12. Scholes, R.J.; Archer, S.R. Tree-grass interactions in savannas. *Annu. Rev. Ecol. Syst.* **1997**, *28*, 517–544. [CrossRef]
13. Stevens, N.; Erasmus, B.F.N.; Archibald, S.; Bond, W.J. Woody encroachment over 70 years in South African savannahs: Overgrazing, global change or extinction aftershock? *Phil. Trans. R. Soc. B* **2016**, *371*, 20150437. [CrossRef]
14. Van Auken, O.W. Causes and consequences of woody plant encroachment into western North American grasslands. *J. Environ. Manag.* **2009**, *90*, 2931–2942. [CrossRef] [PubMed]
15. Zhang, W.; Brandt, M.; Penuelas, J.; Guichard, F.; Tong, X.; Tian, F.; Fensholt, R. Ecosystem structural changes controlled by altered rainfall climatology in tropical savannas. *Nat. Commun.* **2019**, *10*, 671. [CrossRef] [PubMed]
16. Barger, N.N.; Archer, S.R.; Campbell, J.L.; Huang, C.; Morton, J.A.; Knapp, A.K. Woody plant proliferation in North American drylands: A synthesis of impacts on ecosystem carbon balance. *J. Geophys. Res. Biogeosci.* **2011**, *116*, G00K07. [CrossRef]
17. Eldridge, D.J.; Bowker, M.A.; Maestre, F.T.; Roger, E.; Reynolds, J.F.; Whitford, W.G. Impacts of shrub encroachment on ecosystem structure and functioning: Towards a global synthesis. *Ecol. Lett.* **2011**, *14*, 709–722. [CrossRef] [PubMed]
18. Jackson, R.B.; Banner, J.L.; Jobbagy, E.G.; Pockman, W.T.; Wall, D.H. Ecosystem carbon loss with woody plant invasion of grasslands. *Nature* **2002**, *418*, 623–626. [CrossRef] [PubMed]

19. Zhou, Y.; Boutton, T.W.; Ben Wu, X. Soil carbon response to woody plant encroachment: Importance of spatial heterogeneity and deep soil storage. *J. Ecol.* **2017**, *105*, 1738–1749. [CrossRef]
20. Pacala, S.W.; Hurtt, G.C.; Baker, D.; Peylin, P.; Houghton, R.A.; Birdsey, R.A.; Heath, L.; Sundquist, E.T.; Stallard, R.F.; Ciais, P.; et al. Consistent land- and atmosphere-based us carbon sink estimates. *Science* **2001**, *292*, 2316–2320. [CrossRef]
21. Houghton, R.A.; Hackler, J.L. Changes in terrestrial carbon storage in the United States. 1: The roles of agriculture and forestry. *Glob. Ecol. Biogeogr.* **2000**, *9*, 125–144. [CrossRef]
22. Climate Change Science Program. The First State of the Carbon Cycle Report (SOCCR): The North American Carbon Budget and Implications for the Global Carbon Cycle. In *A Report by the U.S. Climate Change Science Program and the Subcommittee on Global Change Research*; King, A.W., Dilling, L., Zimmerman, G.P., Fairman, D.M., Houghton, R.A., Marland, G., Rose, A.Z., Wilbanks, T.J., Eds.; National Oceanic and Atmospheric Administration, National Climatic Data Center: Asheville, NC, USA, 2007.
23. Blaser, W.J.; Shanungu, G.K.; Edwards, P.J.; Venterink, H.O. Woody encroachment reduces nutrient limitation and promotes soil carbon sequestration. *Ecol. Evol.* **2014**, *4*, 1423–1438. [CrossRef]
24. Liao, J.D.; Boutton, T.W.; Jastrow, J.D. Storage and dynamics of carbon and nitrogen in soil physical fractions following woody plant invasion of grassland. *Soil Biol. Biochem.* **2006**, *38*, 3184–3196. [CrossRef]
25. Springsteen, A.; Loya, W.; Liebig, M.; Hendrickson, J. Soil carbon and nitrogen across a chronosequence of woody plant expansion in North Dakota. *Plant Soil* **2010**, *328*, 369–379. [CrossRef]
26. Hughes, R.F.; Archer, S.R.; Asner, G.P.; Wessman, C.A.; McMurtry, C.; Nelson, J.; Ansley, R.J. Changes in aboveground primary production and carbon and nitrogen pools accompanying woody plant encroachment in a temperate savanna. *Glob. Chang. Biol.* **2006**, *12*, 1733–1747. [CrossRef]
27. Li, H.; Shen, H.H.; Chen, L.Y.; Liu, T.Y.; Hu, H.F.; Zhao, X.; Zhou, L.H.; Zhang, P.J.; Fang, J.Y. Effects of shrub encroachment on soil organic carbon in global grasslands. *Sci. Rep.* **2016**, *6*, 28974. [CrossRef] [PubMed]
28. Schlesinger, W.H.; Raikes, J.A.; Hartley, A.E.; Cross, A.E. On the spatial pattern of soil nutrients in desert ecosystems. *Ecology* **1996**, *77*, 364–374. [CrossRef]
29. Boutton, T.W.; Archer, S.R.; Midwood, A.J.; Zitzer, S.F.; Bol, R. δ^{13}C values of soil organic carbon and their use in documenting vegetation change in a subtropical savanna ecosystem. *Geoderma* **1998**, *82*, 5–41. [CrossRef]
30. Dzurec, R.; Boutton, T.; Caldwell, M.; Smith, B. Carbon isotope ratios of soil organic matter and their use in assessing community composition changes in Curlew Valley, Utah. *Oecologia* **1985**, *66*, 17–24. [CrossRef]
31. Victoria, R.L.; Fernandes, F.; Martinelli, L.A.; Piccolo, M.D.C.; Decamargo, P.B.; Trumbore, S. Past vegetation changes in the Brazilian pantanal arboreal–grassy savanna ecotone by using carbon isotopes in the soil organic matter. *Glob. Chang. Biol.* **1995**, *1*, 165–171. [CrossRef]
32. Balesdent, J.; Girardin, C.; Mariotti, A. Site-δ^{13}C of tree leaves and soil organic matter in a temperate forest. *Ecology* **1993**, *74*, 1713–1721. [CrossRef]
33. Boutton, T.W. Stable carbon isotope ratios of organic matter and their use as indicators of vegetation and climate changes. In *Mass Spectrometry of Soils*; Boutton, T.W., Yamasaki, S.I., Eds.; Marcel Dekker, Inc.: New York, NY, USA, 1996; pp. 47–82.
34. Breecker, D.O.; Bergel, S.; Nadel, M.; Tremblay, M.M.; Osuna-Orozco, R.; Larson, T.E.; Sharp, Z.D. Minor stable carbon isotope fractionation between respired carbon dioxide and bulk soil organic matter during laboratory incubation of topsoil. *Biogeochemistry* **2015**, *123*, 83–98. [CrossRef]
35. Ehleringer, J.R.; Buchmann, N.; Flanagan, L.B. Carbon isotope ratios in belowground carbon cycle processes. *Ecol. Appl.* **2000**, *10*, 412–422. [CrossRef]
36. Lerch, T.Z.; Nunan, N.; Dignac, M.F.; Chenu, C.; Mariotti, A. Variations in microbial isotopic fractionation during soil organic matter decomposition. *Biogeochemistry* **2011**, *106*, 5–21. [CrossRef]
37. Bai, E.; Boutton, T.W.; Wu, X.B.; Liu, F.; Archer, S.R. Landscape-scale vegetation dynamics inferred from spatial patterns of soil δ^{13}C in a subtropical savanna parkland. *J. Geophys. Res. Biogeosci.* **2009**, *114*, G01019. [CrossRef]
38. Biedenbender, S.H.; McClaran, M.P.; Quade, J.; Weltz, M.A. Landscape patterns of vegetation change indicated by soil carbon isotope composition. *Geoderma* **2004**, *119*, 69–83. [CrossRef]
39. Freier, K.P.; Glaser, B.; Zech, W. Mathematical modeling of soil carbon turnover in natural *Podocarpus* forest and *Eucalyptus* plantation in Ethiopia using compound specific δ^{13}C analysis. *Glob. Chang. Biol.* **2010**, *16*, 1487–1502. [CrossRef]

40. Liao, J.D.; Boutton, T.W.; Jastrow, J.D. Organic matter turnover in soil physical fractions following woody plant invasion of grassland: Evidence from natural ^{13}C and ^{15}N. *Soil Biol. Biochem.* **2006**, *38*, 3197–3210. [CrossRef]
41. Puttock, A.; Dungait, J.A.J.; Bol, R.; Dixon, E.R.; Macleod, C.J.A.; Brazier, R.E. Stable carbon isotope analysis of fluvial sediment fluxes over two contrasting C_4-C_3 semi-arid vegetation transitions. *Rapid Commun. Mass Spectrom.* **2012**, *26*, 2386–2392. [CrossRef]
42. Krull, E.; Bray, S.; Harms, B.; Baxter, N.; Bol, R.; Farquhar, G. Development of a stable isotope index to assess decadal-scale vegetation change and application to woodlands of the Burdekin catchment, Australia. *Glob. Change Biol.* **2007**, *13*, 1455–1468. [CrossRef]
43. Turnbull, L.; Brazier, R.E.; Wainwright, J.; Dixon, L.; Bol, R. Use of carbon isotope analysis to understand semi-arid erosion dynamics and long-term semi-arid land degradation. *Rapid Commun. Mass Spectrom.* **2008**, *22*, 1697–1702. [CrossRef]
44. Pringle, R.M.; Doak, D.F.; Brody, A.K.; Jocque, R.; Palmer, T.M. Spatial pattern enhances ecosystem functioning in an African savanna. *PloS Biol.* **2010**, *8*, e1000377. [CrossRef]
45. Ettema, C.H.; Wardle, D.A. Spatial soil ecology. *Trends Ecol. Evol.* **2002**, *17*, 177–183. [CrossRef]
46. Liu, F.; Wu, X.B.; Bai, E.; Boutton, T.W.; Archer, S.R. Quantifying soil organic carbon in complex landscapes: An example of grassland undergoing encroachment of woody plants. *Glob. Chang. Biol.* **2011**, *17*, 1119–1129. [CrossRef]
47. Loescher, H.; Ayres, E.; Duffy, P.; Luo, H.Y.; Brunke, M. Spatial variation in soil properties among North American ecosystems and guidelines for sampling designs. *PLoS ONE* **2014**, *9*, e83216. [CrossRef] [PubMed]
48. Biggs, T.H.; Quade, J.; Webb, R.H. $\delta^{13}C$ values of soil organic matter in semiarid grassland with mesquite (*Prosopis*) encroachment in southeastern Arizona. *Geoderma* **2002**, *110*, 109–130. [CrossRef]
49. van Kessel, C.; Farrell, R.E.; Pennock, D.J. Carbon-13 and nitrogen-15 natural-abundance in crop residues and soil organic-matter. *Soil Sci. Soc. Am. J.* **1994**, *58*, 382–389. [CrossRef]
50. Zhou, Y.; Boutton, T.W.; Wu, X.B. Woody plant encroachment amplifies spatial heterogeneity of soil phosphorus to considerable depth. *Ecology* **2018**, *99*, 136–147. [CrossRef]
51. Archer, S. Tree-grass dynamics in a *Prosopis*-thornscrub savanna parkland: Reconstructing the past and predicting the future. *Ecoscience* **1995**, *2*, 83–99. [CrossRef]
52. Archer, S.; Scifres, C.; Bassham, C.; Maggio, R. Autogenic succession in a subtropical savanna: Conversion of grassland to thorn woodland. *Ecol. Monogr.* **1988**, *58*, 111–127. [CrossRef]
53. Zhou, Y.; Boutton, T.W.; Wu, X.B.; Yang, C.H. Spatial heterogeneity of subsurface soil texture drives landscape-scale patterns of woody patches in a subtropical savanna. *Landsc. Ecol.* **2017**, *32*, 915–929. [CrossRef]
54. Zhou, Y.; Watts, S.E.; Boutton, T.W.; Archer, S.R. Root density distribution and biomass allocation of co-occurring woody plants on contrasting soils in a subtropical savanna parkland. *Plant Soil* **2019**, *438*, 263–279. [CrossRef]
55. U.S.D.A. Soil Conservation Service. *Soil Survey of Jim Wells County, Texas*; Soil Conservation Service: Washington, DC, USA, 1979.
56. Loomis, L.E. Influence of Heterogeneous Subsoil Development on Vegetation Patterns in a Subtropical Savanna Parkland, Texas. Ph.D. Dissertation, Texas A&M University, College Station, TX, USA, 1989.
57. Whittaker, R.; Gilbert, L.; Connell, J. Analysis of a two-phase pattern in a mesquite grassland, Texas. *J. Ecol.* **1979**, 935–952. [CrossRef]
58. Bai, E.; Boutton, T.W.; Liu, F.; Wu, X.B.; Archer, S.R. Spatial patterns of soil $\delta^{13}C$ reveal grassland-to-woodland successional processes. *Org. Geochem.* **2012**, *42*, 1512–1518. [CrossRef]
59. McCulley, R.L.; Archer, S.R.; Boutton, T.W.; Hons, F.M.; Zuberer, D.A. Soil respiration and nutrient cycling in wooded communities developing in grassland. *Ecology* **2004**, *85*, 2804–2817. [CrossRef]
60. Zhou, Y.; Boutton, T.W.; Wu, X.B. Soil phosphorus does not keep pace with soil carbon and nitrogen accumulation following woody encroachment. *Glob. Chang. Biol.* **2018**, *24*, 1992–2007. [CrossRef] [PubMed]
61. Turner, M.G.; Gardner, R.H.; O'Neill, R.V. *Landscape Ecology in Theory and Practice*; Springer: New York, NY, USA, 2001. [CrossRef]

62. Boutton, T.W.; Liao, J.D.; Filley, T.; Archer, S.R. Belowground carbon storage and dynamics accompanying woody plant encroachment in a subtropical savanna. In *Soil Carbon Sequestration and the Greenhouse Effect*, 2nd ed.; Lal, R., Follett, R., Eds.; Soil Science Society of America: Madison, WI, USA, 2009; pp. 181–205. [CrossRef]
63. Harris, D.; Horwath, W.R.; van Kessel, C. Acid fumigation of soils to remove carbonates prior to total organic carbon or ^{13}C isotopic analysis. *Soil Sci. Soc. Am. J.* **2001**, *65*, 1853–1856. [CrossRef]
64. Bostrom, B.; Comstedt, D.; Ekblad, A. Isotope fractionation and ^{13}C enrichment in soil profiles during the decomposition of soil organic matter. *Oecologia* **2007**, *153*, 89–98. [CrossRef]
65. Wynn, J.G.; Bird, M.I. C_4-derived soil organic carbon decomposes faster than its C_3 counterpart in mixed C_3/C_4 soils. *Glob. Chang. Biol.* **2007**, *13*, 2206–2217. [CrossRef]
66. Ampleman, M.D.; Crawford, K.M.; Fike, D.A. Differential soil organic carbon storage at forb- and grass-dominated plant communities, 33 years after tallgrass prairie restoration. *Plant Soil* **2014**, *374*, 899–913. [CrossRef]
67. Saiz, G.; Bird, M.; Wurster, C.; Quesada, C.A.; Ascough, P.; Domingues, T.; Schrodt, F.; Schwarz, M.; Feldpausch, T.R.; Veenendaal, E.; et al. The influence of C_3 and C_4 vegetation on soil organic matter dynamics in contrasting semi-natural tropical ecosystems. *Biogeosciences* **2015**, *12*, 5041–5059. [CrossRef]
68. Littell, R.C.; Milliken, G.A.; Stroup, W.W.; Wolfinger, R.D.; Oliver, S. *SAS for Mixed Models*; SAS Institute: Cary, NC, USA, 2006.
69. R Core Team. R: A language and environment for statistical computing. R Foundation for Statistical Computing: Vienna, Austria. Available online: https://www.R-project.org/ (accessed on 12 November 2019).
70. Throop, H.L.; Archer, S.R. Shrub (*Prosopis velutina*) encroachment in a semidesert grassland: Spatial-temporal changes in soil organic carbon and nitrogen pools. *Glob. Chang. Biol.* **2008**, *14*, 2420–2431. [CrossRef]
71. Rasse, D.P.; Rumpel, C.; Dignac, M.F. Is soil carbon mostly root carbon? Mechanisms for a specific stabilisation. *Plant Soil* **2005**, *269*, 341–356. [CrossRef]
72. Rumpel, C.; Kogel-Knabner, I. Deep soil organic matter-a key but poorly understood component of terrestrial C cycle. *Plant Soil* **2011**, *338*, 143–158. [CrossRef]
73. Schmidt, M.W.I.; Torn, M.S.; Abiven, S.; Dittmar, T.; Guggenberger, G.; Janssens, I.A.; Kleber, M.; Kogel-Knabner, I.; Lehmann, J.; Manning, D.A.C.; et al. Persistence of soil organic matter as an ecosystem property. *Nature* **2011**, *478*, 49–56. [CrossRef] [PubMed]
74. Jackson, R.B.; Canadell, J.; Ehleringer, J.R.; Mooney, H.A.; Sala, O.E.; Schulze, E.D. A global analysis of root distributions for terrestrial biomes. *Oecologia* **1996**, *108*, 389–411. [CrossRef] [PubMed]
75. Schenk, H.J.; Jackson, R.B. Rooting depths, lateral root spreads and below-ground/above-ground allometries of plants in water-limited ecosystems. *J. Ecol.* **2002**, *90*, 480–494. [CrossRef]
76. Stoker, R.L. An Object-Oriented, Spatially-Explicit Simulation Model of Vegetation Dynamics in a South Texas Savanna. Ph.D. Thesis, Texas A&M University, College Station, TX, USA, 1998.
77. Archer, S.; Smeins, F. Ecosystem-level processes. In *Grazing Management: An Ecological Perspective*; Heitschmidt, R.K., Stuth, J.W., Eds.; Timber Press: Portland, OR, USA, 1991; pp. 109–140.
78. Augustine, D.J.; Derner, J.D.; Milchunas, D.; Blumenthal, D.; Porensky, L.M. Grazing moderates increases in C_3 grass abundance over seven decades across a soil texture gradient in shortgrass steppe. *J. Veg. Sci.* **2017**, *28*, 562–572. [CrossRef]
79. Wang, Y.; Amundson, R.; Trumbore, S. Radiocarbon dating of soil organic matter. *Quat. Res.* **1996**, *45*, 282–288. [CrossRef]
80. Polley, H.W.; Mayeux, H.S.; Johnson, H.B.; Tischler, C.R. Viewpoint: Atmospheric CO_2, soil water, and shrub/grass ratios on rangelands. *J. Range Manag.* **1997**, *50*, 278–284. [CrossRef]
81. NOAA National Centers for Environmental Information. Climate at a Glance: County Mapping. 2019. Available online: https://www.ncdc.noaa.gov/cag/county/mapping (accessed on 14 October 2019).
82. Venter, Z.S.; Cramer, M.D.; Hawkins, H.J. Drivers of woody plant encroachment over Africa. *Nat. Commun.* **2018**, *9*, 2272. [CrossRef]
83. Osborne, C.P.; Charles-Dominique, T.; Stevens, N.; Bond, W.J.; Midgley, G.; Lehmann, C.E.R. Human impacts in African savannas are mediated by plant functional traits. *New Phytol.* **2018**, *220*, 10–24. [CrossRef]
84. Creamer, C.A.; Filley, T.R.; Boutton, T.W. Long-term incubations of size and density separated soil fractions to inform soil organic carbon decay dynamics. *Soil Biol. Biochem.* **2013**, *57*, 496–503. [CrossRef]

85. Filley, T.R.; Boutton, T.W.; Liao, J.D.; Jastrow, J.D.; Gamblin, D.E. Chemical changes to nonaggregated particulate soil organic matter following grassland-to-woodland transition in a subtropical savanna. *J. Geophys. Res. Biogeosci.* **2008**, *113*, G03009. [CrossRef]
86. Kantola, I.B. Biogeochemistry of Woody Plant Invasion: Phosphorus Cycling and Microbial Community Composition. Ph.D. Thesis, Texas A&M University, College Station, TX, USA, 2012.
87. Hibbard, K.A.; Schimel, D.S.; Archer, S.; Ojima, D.S.; Parton, W. Grassland to woodland transitions: Integrating changes in landscape structure and biogeochemistry. *Ecol. Appl.* **2003**, *13*, 911–926. [CrossRef]
88. Liao, J.D.; Boutton, T.W. Soil microbial biomass response to woody plant invasion of grassland. *Soil Biol. Biochem.* **2008**, *40*, 1207–1216. [CrossRef]
89. Creamer, C.A.; Filley, T.R.; Boutton, T.W.; Rowe, H. Grassland to woodland transitions: Dynamic response of microbial community structure and carbon use patterns. *J. Geophys. Res. Biogeosci.* **2016**, *121*, 1675–1688. [CrossRef]
90. Hollister, E.B.; Schadt, C.W.; Palumbo, A.V.; Ansley, R.J.; Boutton, T.W. Structural and functional diversity of soil bacterial and fungal communities following woody plant encroachment in the southern Great Plains. *Soil Biol. Biochem.* **2010**, *42*, 1816–1824. [CrossRef]
91. Biederman, L.; Boutton, T.W. Spatial variation in biodiversity and trophic structure of soil nematode communities in a subtropical savanna parkland: Responses to woody plant encroachment. *Appl. Soil Ecol.* **2010**, *46*, 168–176. [CrossRef]
92. Luvuno, L.; Biggs, R.; Stevens, N.; Esler, K. Woody encroachment as a social-ecological regime shift. *Sustainability* **2018**, *10*, 2221. [CrossRef]
93. Wilcox, B.P.; Birt, A.; Archer, S.R.; Fuhlendorf, S.D.; Kreuter, U.P.; Sorice, M.G.; Van Leeuwen, W.J.D.; Zou, C.B. Viewing woody plant encroachment through a social-ecological lens. *BioScience* **2018**, *68*, 691–705. [CrossRef]

Table S1

Soil physical characteristics and root densities for grasslands, clusters, and groves. Each value is a mean, where the number of samples is: grasslands = 200, clusters = 41, and groves = 79. Data are extracted from previous publications [19,53] at this study area.

Soil Depth (cm)	pH	Soil Bulk Density (g cm^{-3})	Particle Size Distribution			Fine Root Density (kg m^{-3})	Total Root Density (kg m^{-3})
			Sand (%)	Silt (%)	Clay (%)		
Grasslands							
0-5	7.34	1.34	76.4	10.8	12.8	3.5	3.8
5-15	7.21	1.44	74.5	10.1	15.4	2.2	2.2
15-30	7.17	1.41	71.5	10.7	17.8	1.4	1.9
30-50	7.30	1.46	67.2	11.1	21.7	1.0	1.0
50-80	7.54	1.52	62.9	12.2	25.0	0.5	0.5
80-120	7.74	1.62	55.8	14.1	30.1	0.3	0.3
Clusters							
0-5	7.34	1.10	75.4	11.1	13.5	10.1	21.3
5-15	7.34	1.29	74.1	10.7	15.2	5.4	16.6
15-30	7.35	1.36	71.4	11.1	17.5	2.7	11.0
30-50	7.46	1.43	67.8	11.3	20.9	1.8	3.1
50-80	7.65	1.49	63.0	12.2	24.9	0.9	2.0
80-120	7.79	1.59	55.8	14.0	30.6	0.6	0.8
Groves							
0-5	7.39	1.06	75.0	11.8	13.2	10.2	16.0
5-15	7.48	1.31	73.3	11.2	15.5	5.8	11.8
15-30	7.54	1.37	70.4	11.7	17.9	3.1	10.6
30-50	7.64	1.43	68.1	11.9	20.0	1.9	4.0
50-80	7.74	1.47	64.9	12.2	22.9	1.1	4.2
80-120	7.82	1.59	59.0	13.5	27.6	0.8	1.5

Table S2

$\delta^{13}C$ values (‰ vs. V-PDB) of leaf and fine root tissues of dominant plant species across the 160 m × 100 m landscape in a subtropical savanna ecosystem. For each woody species, approximately equal amounts of leaves from three individuals were collected to make a composite sample; then, fine roots were excavated from surface soils after confirming their linkages to the selected three individuals and mixed to create a composite sample. The same sampling method was applied to forbs and grasses, but more than three individuals were sampled for each species in order to meet the mass requirements for elemental and isotopic analyses. Number of woody plant species = 15, forbs = 9, and grasses = 13.

Species name	**$\delta^{13}C$ values (‰)**	
	Leaf tissue	**Fine root tissue**
Woody plant species		
Bernardia myricifolia	-27.1	-26.1
Celtis pallida	-30.9	-30.0
Condalia hookeri	-30.4	-28.5
Diospyros texana	-29.0	-25.9
Foresteria angustifolia	-29.5	-26.5
Karwinskia humboldtiana	-28.7	-27.0
Lycium berlandieri	-28.1	-27.1
Mahonia trifoliolata	-26.2	-25.7
Schaefferia cuneifolia	-29.5	-27.5
Zanthoxylum fagara	-28.7	-27.9
Coleogyne ramosissima	-28.2	-27.5
Salvia ballotiflora	-30.2	-27.6
Acacia greggii	-28.7	-26.4
Acacia schaffneri	-29.9	-28.3
Prosopis glandulosa	-27.8	-25.6
Forbs		
Croton texensis	-29.6	-27.8
Wedelia texana	-29.8	-27.6
Aphanostephus riddellii	-30.7	-27.9
Ambrosia confertiflora	-29.5	-27.5
Parthenium hysterophorus	-30.0	-28.3
Palafoxia callosa	-28.6	-27.5
Amphiachyris amoena	-28.6	-27.5
Thymophylla pentachaeta	-28.9	-27.9
Xanthisma texanum	-29.3	-26.9
Grasses		
Tridens albescens	-13.9	-14.4
Setaria texana	-13.0	-12.7
Bothriochloa ischaemum	-11.6	-12.4
Aristida purpurea	-12.4	-12.5
Cenchrus ciliaris	-11.8	-12.2

Heteropogon contortus	-12.5	-11.6
Chloris cucullata	-14.4	-12.7
Eragrostis secundiflora	-12.3	-12.4
Paspalum setaceum	-12.5	-11.2
Sporobolus neglectus	-13.8	-12.5
Bouteloua rigidiseta	-14.3	-13.8
Bouteloua trifida	-14.2	-13.3
Panicum hallii	-13.0	-13.2

Table S3

Descriptive statistics for all soil $\delta^{13}C$ values (‰ vs. V-PDB) across the 160 m × 100 m landscape within each depth increment. Number of samples, n = 320.

	0-5 cm	5-15 cm	15-30 cm	30-50 cm	50-80 cm	80-120 cm
Mean	-22.0	-19.4	-16.8	-16.1	-16.2	-17.3
Median	-21.7	-18.9	-16.3	-15.7	-16.1	-17.2
Minimum	-27.3	-24.7	-21.6	-21.6	-20.2	-23.0
Maximum	-17.7	-15.7	-14.3	-13.7	-14.1	-15.1
Standard deviation	2.2	2.0	1.5	1.3	1.0	1.0
Standard error	0.1	0.1	0.1	0.1	0.1	0.1
Coefficient of variation	-9.78	-10.13	-9.19	-8.20	-6.06	-5.57
Skewness	-0.31	-0.55	-0.88	-1.38	-0.69	-1.17
Range	9.6	8.9	7.3	7.9	6.1	7.9

Figure S1

Root densities (kg m^{-3}) within landscape elements to a depth of 1 m. Number of samples: grassland = 200, cluster = 41, and grove = 79. Mid-points of each soil depth increment (e.g. 2.5 cm for 0-5 cm soil depth increment) were used to fit the exponential models.

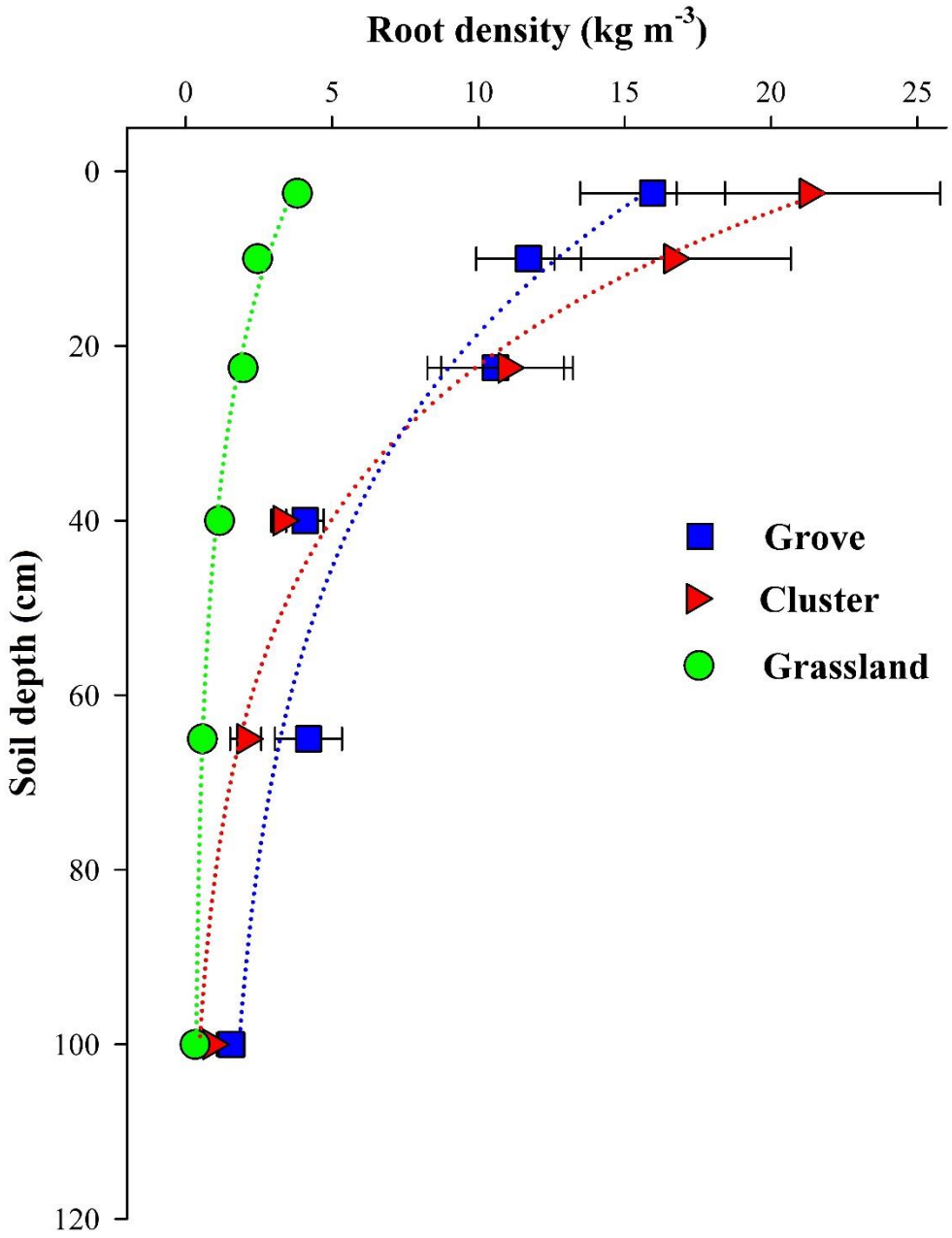

Figure S2

Relationships between soil $\delta^{13}C$ (‰ vs. V-PDB) and root density (kg C m^{-3}, log_{10}-transformed) throughout the soil profile. Number of samples: grassland = 200, cluster = 41, and grove = 79. Note that scales are different.